Available online at www.sciencedirect.com
SCIENCE DIRECT®
Physics Letters B 624 (2005) 203–209
PHYSICS LETTERS B
www.elsevier.com/locate/physletb

Electron scattering on halo nuclei

C.A. Bertulani

Department of Physics, University of Arizona, 1118 E 4th St., Tucson, AZ 85721, USA

Received 21 March 2005; received in revised form 11 July 2005; accepted 5 August 2005

Available online 19 August 2005

Editor: W. Haxton

Abstract

The inelastic scattering of electrons on weakly-bound nuclei is studied with a simple model based on the long range behavior of the bound state wavefunction and on the effective-range expansion for the continuum wavefunctions. Three mechanisms have been considered: (a) dissociation of halo nuclei by high energy electrons, (b) dissociation by electrons present in a fixed target, and (c) Coulomb dissociation. It is shown that the properties of halo nuclei can be studied in electron-radioactive beam colliders using the electro-disintegration process. A comparison with fixed-target experiments is also performed.

PACS: 25.30.Fj; 25.60.Gc

1. Introduction

A study of properties of weakly-bound neutron-rich, or halo nuclei, has been carried out intensively worldwide during the last decades [1]. Because of their short beta-decay lifetimes, halo nuclei are often studied in fragmentation facilities, where they are produced in-flight. The probes are hadronic, usually stable nuclear targets. Typically, one uses Coulomb dissociation, stripping, elastic scattering, etc., [2] as nuclear structure probes. Such studies are complicated because the reaction mechanisms are not as well understood as with stable nuclear projectiles. The use of electromagnetic probes, e.g., electron scattering, is thus highly desirable. In fact, new experimental facilities for electron-scattering on unstable nuclear beams are under construction [3]. An accurate determination of charge distributions in exotic nuclei can be obtained with electrons using inverse kinematics in a electron-nucleus collider mode [3]. Electronic excitation, or dissociation, of nuclear beams can also be exploited for a deeper understanding of their structure.

It is the aim of this work to explore basic results of electron scattering on the simplest of all nuclear halo structures, namely, a one-neutron halo system. The physics mechanisms and the conditions for the realization of electron scattering experiments are assessed. Such study has also an impact in nuclear astrophysics

E-mail address: bertulani@physics.arizona.edu (C.A. Bertulani).

0370-2693/$ – see front matter
doi:10.1016/j.physletb.2005.08.030

as it allows to deduce what are the lowest binding energies of halo nuclei possible in stellar environments, where free electrons are available.

A high energy beam of weakly-bound neutron-rich nuclei dissociates as it penetrates a target due to the interaction with the atomic electrons. Since a heavy element target, e.g., ^{208}Pb, contains almost 100 electrons, the dissociation cross sections are large, assuming that each electron in the atom scatters independently on the projectile. Moreover, due to the atomic orbital motion, the innermost electrons have large relative energy with the incoming nucleus, increasing the dissociation probability. This process is of crucial importance in designing experiments aiming at studying properties of halo nuclei with the Coulomb dissociation method.

The dissociation of neutron-rich nuclei, with small neutron separation energies, in stars can impose stringent limits on the stellar scenario where these nuclei play a role. For example, if the r-process proceeds partially out of equilibrium, the neutron radiative capture cross sections would have to be large enough to match the electron dissociation cross sections, with the appropriate neutron and electron density weights.

2. Electron scattering on neutron halo nuclei

I will consider the process $e + a \to e' + b + c$ at small momentum transfers, $\mathbf{q} = (\mathbf{p}' - \mathbf{p})/\hbar$, such that $qR \ll 1$ (R is the nuclear size). For simplicity, particle b is taken as a neutron and c as a core (inert) nucleus. The results obtained here are general and can be easily extended to the case of two-neutron halos.

The differential cross section for this process is given by [4]

$$\frac{d\sigma_e}{d\Omega} = \frac{2e^2}{(\hbar c)^4}\left(\frac{p'}{p}\right)\frac{2J_f+1}{2J_i+1}\frac{EE' + c^2\mathbf{p}\cdot\mathbf{p}' + m_e^2c^4}{q^4} \times \left|\rho_{fi}(\mathbf{q})\right|^2 N_f, \tag{1}$$

where E (E') and $\mathbf{p}$ ($\mathbf{p}'$) are the initial (final) energy and momentum of the electron, respectively. J_i (J_f) is the initial (final) nuclear spin, and N_f is the density of final states of the nucleus. The nuclear form factor $\rho_{fi}(q)$ is given by

$$\rho_{fi}(\mathbf{q}) = \int \rho_{fi}(\mathbf{r}) e^{i\mathbf{q}\cdot\mathbf{r}}\, d^3r, \tag{2}$$

where $\rho_{fi}(\mathbf{r}) = \psi_f^*\,\psi_i$ is the nuclear charge transition density, with ψ_i (ψ_f) equal to the initial (final) nuclear wavefunction. The cross section given by Eq. (1) only includes longitudinal (also called Coulomb) excitations, dominant at low energy transfers [5–7].

Eq. (1) is based on the first Born approximation. It gives good results for light nuclei (e.g., ^{12}C) and high-energy electrons. For large-Z nuclei the agreement with experiments is only of a qualitative nature. The effects of the distortion of the electron waves have been studied by many authors (see, e.g., Refs. [8,9]). For a rough estimate of this effect, I follow Ref. [10]. For transition densities peaked at the nuclear surface with radius R_0, the correction due to Coulomb distortion is approximately given by

$$Q = \frac{d\sigma_{\rm Born}/d\Omega}{d\sigma_{\rm Corrected}/d\Omega} \simeq \frac{1}{1+\beta Ze^2/\hbar c}, \tag{3}$$

with

$$\beta = \frac{120}{x^2}\left\{-\frac{1}{160x^3}\left[1+\frac{3}{2}\cos(2x)+3x\sin(2x) + \frac{x^2}{3}\big(4+5\cos(2x)\big)+\frac{10}{3}x^3\sin(2x)\right] + \frac{x}{60}\left[\frac{9}{4}-\cos(2x)\right]+\frac{x^2}{60}\big[\pi-2\,\mathrm{Si}(2x)\big] + n_1(2x)\left[\frac{1}{16x}+\frac{x}{40}\right]\right\}, \tag{4}$$

where $x = pR_0/\hbar$, Si is the sine integral, $\mathrm{Si}(x) = \int_0^\infty dt\,\sin t/t$, and $n_i(x)$ is the spherical Bessel function of the second kind. The above result is valid for monopole ($l = 0$) transitions. Corresponding expressions for higher order transitions are found in Ref. [10].

Table 1 shows the correction due to Coulomb distortion, Eq. (3), for ^{11}Li and ^{19}C targets and several electron kinetic energies K_e. One sees that below

Table 1
The Coulomb correction factor, Eq. (3), for electron scattering on ^{11}Li and ^{19}C and for several kinetic energies, K_e (in MeV)

K_e [MeV]	Q (^{11}Li)	Q (^{19}C)
0.1	0.879	0.784
1	0.880	0.786
10	0.887	0.797
10^2	0.949	0.903
10^3	0.994	0.989

$K_e = 100$ MeV it is important to account for Coulomb distortion of the electronic waves. A radius $R_0 = 3.5$ fm was assumed for both nuclei. The Coulomb distortion correction decreases approximately linearly with R_0.

An additional correction, due to nuclear recoil [4], changes Eq. (1) by a factor $f_{\rm rec} \simeq 1 + (2E_x/Mc^2) \times \sin(\theta/2)$, where E_x is the excitation energy, M is the nuclear mass, and θ is the electron scattering angle. For the dissociation of weakly-bound nuclei, $E_x \ll Mc^2$ and this correction is much less relevant than the distortion of the electronic waves. I will neglect the Coulomb distortion and recoil effects from here on, bearing in mind that they should be taken into account in a more precise calculation.

In a simplified model for the halo nucleus the radial parts of the initial and final wavefunctions are represented by single-particle states of the form

$$u_i(r) = A_i h_{l_i}(i\eta r),$$
$$u_f(r) = \cos(\delta_{l_f}) j_{l_f}(kr) - \sin(\delta_{l_f}) n_{l_f}(kr) \tag{5}$$

where η is related to the neutron separation energy $S_n = \hbar^2\eta^2/2\mu$. $h_{l_i}(i\eta r)$ represents the large distance behavior of the bound state wavefunction, μ is the reduced mass of the neutron + core system and $\hbar k$ their relative momentum in the final state. h_{l_i}, j_{l_f}, and n_{l_f} are the spherical Hankel, Bessel, and Neumann functions, respectively. A_i is the ground state asymptotic normalization coefficient, which includes the normalization of the neutron single-particle wavefunction, and a spectroscopic factor which accounts for the many-body aspects. This single-particle picture has been used previously to study Coulomb excitation of halo nuclei with success [11–16].

The constant A_i (with spectroscopic factor equal to the unity) is used to normalize the bound state wavefunction, and corrects for the nuclear interaction range, r_0. In the case of an s-wave ground state ($l_i = 0$), one has [17] $A_i = \exp(\eta r_0)\sqrt{\eta/2\pi(1+\eta r_0)}$. For weakly-bound nuclei, $1/\eta \gg r_0$ and $A_i \simeq \sqrt{\eta/2\pi}$. The ground state wavefunction entering the transition density integral, Eq. (2), is well represented by the Hankel function $h_{l_i}(i\eta r)$. Note that the wavefunctions in Eq. (5) are not orthonormal. However, the transition density matrix elements of relevance for Coulomb excitation (and similarly for electron scattering) are dominated by the outside region ($r > R$) [13,14]. Far from a resonance, the continuum wavefunction $u_f(r)$ is small inside the nuclear radius. Its asymptotic dependence is well described by Eq. (5).

Using Eq. (5) the form factor in Eq. (2) can be calculated analytically by expanding $e^{i\mathbf{q}\cdot\mathbf{r}}$ into multipoles. The results will depend on the parameters S_n, R, and δ_{l_f}. To eliminate the dependence on R, the lower limit of the radial integral in Eq. (2) is extended to $r = 0$. The results for an s-wave ground state and the lowest order continuum angular momenta ($l_f = 0, 1, 2$) are particularly simple. They are:

$$\rho^{(0)}_{fi}(q) = \frac{e^{(0)}_{\rm eff}\pi A_i}{qk}\left\{L - \frac{2k}{-1/a_0 + r_0k^2/2}M\right\},$$
$$\rho^{(1)}_{fi}(q) = \frac{e^{(1)}_{\rm eff} i\pi A_i}{q^2k^2}\left\{\frac{\eta^2+k^2+q^2}{2}L - 2qk - \frac{k^3}{-1/a_1 + r_1k^2/2} \times \left[2\eta q + \left(\eta^2+k^2+q^2\right)M\right]\right\},$$
$$\rho^{(2)}_{fi}(q) = \frac{e^{(2)}_{\rm eff}\pi A_i}{4k^3q^3}\left\{8kq\left(\eta^2+k^2+q^2\right) - \frac{3k^4 + 3(\eta^2+q^2)^2 + 2k^2(3\eta^2+q^2)}{2}L + \frac{k^5}{-1/a_2 + r_2k^2/2}\left[6\eta\left(k^2+\eta^2\right)q + 10\eta q^3 + \left(3k^4 + 3\left(\eta^2+q^2\right)^2 + 2k^2\left(3\eta^2+q^2\right)\right)M\right]\right\}, \tag{6}$$

where

$$L = \ln\left(\frac{\eta^2+(k+q)^2}{\eta^2+(k-q)^2}\right),$$
$$M = \tan^{-1}\left(\frac{k-q}{\eta}\right) - \tan^{-1}\left(\frac{k+q}{\eta}\right). \tag{7}$$

In these equations $e^{(\lambda)}_{\rm eff} = eZ(-1/A)^\lambda$ is the neutron-core effective charge which depends on the transition multipolarity λ ($\lambda = l_f$ for $l_i = 0$). The effective range approximation $k^{2l+1}\cot\delta_l = -1/a_l + r_lk^2/2$ has been used, where the parameters a_l and r_l are the scattering length and the effective range, respectively. Notice that only for $l = 0$ the scattering length and effective range have dimensions of length.

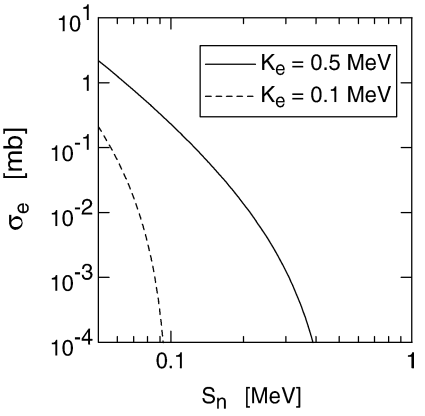

Fig. 1. Cross sections for electron induced breakup as a function of the separation energy, S_n, and for electron bombarding energies equal to 0.1 (dashed) and 0.5 MeV (solid).

The $l = 0$ form factor has a large sensitivity to the orthogonality of the wavefunctions. If one assumes a zero-range potential for the neutron-core interaction, the scattering wavefunction, orthogonal to the bound-state wavefunction, is given by $\psi_{\mathbf{k}}^{(+)}(\mathbf{r}) = \exp(i\mathbf{k}\cdot\mathbf{r}) - \exp(ikr)/[(\eta + ik)r]$. The s-wave scattering length is then just $a_0 = 1/\eta$. Using this value, together with $r_0 = 0$, in the equation for $\rho_{fi}^{(0)}(q)$ leads to a large cancellation between the first and second terms. The $l = 1, 2$ form factors are also very sensitive to the scattering lengths and effective ranges. For example using $a_1 \simeq 5$ fm^3 and $r_1 = 0$ fm^{-1} reduces the magnitude of $\rho_{fi}^{(1)}(q)$ by 10% for scattering at forward angles. These results show that it is very important to include the correct energy dependence of the phase-shifts to obtain an accurate description of electron scattering off halo nuclei [16].

In what follows, I will use $e_{\rm eff}^{(\lambda)} = e$, $R = 0$, $\mu = m_N$ (nucleon mass), and neglect the terms containing the effective-range expansion parameters in Eq. (6). These approximations are not necessary but, with these choices, the numerical results will not depend on the charges and mass parameters of a particular nucleus; only on its neutron separation energy S_n.

The total electron-disintegration cross section is obtained from Eq. (1), with the density of states given by $N_f = d^3k/(2\pi)^3$, and integrating over $\mathbf{k}$ and Ω. Fig. 1 shows the electro-dissociation cross sections obtained by a numerical integration of Eq. (1), as a function of the separation energy, S_n, for electron bombarding energies equal to 0.1 and 0.5 MeV, respectively. One observes that only for very low neutron separation energies ($S_n \lesssim 50$ keV) the electro-disintegration cross section becomes larger than 1 mb. If a more realistic model for $l = 1$ transitions is used, the cross section will be further reduced by: (a) a factor $(Z_a/A_a)^2 \lesssim 1/4$ due to the effective charge, (b) by properly orthogonalized wavefunctions, and (c) by the energy dependence of the phase-shifts.

Fig. 1 also shows that the electron dissociation cross section increases appreciably with the electron energy. It is thus instructive to study the dependence of the cross section on the electron energy at high energies. The electron energy will be considered to be much larger than the energy transfer in the dissociation, i.e., $E \gg \Delta E = E_x$ (E_x denotes the excitation energy). The scattering is peaked at forward angles and, from kinematics, $q = k'\cos\theta - k \simeq \Delta k \simeq E_x/\hbar c$. For energy transfers E_x of the order of a few MeV, one also has $q \ll p, \eta$. Using Eqs. (6) one obtains for the leading multipolarity ($l = 1$)

$$\rho_{fi}^{(1)}(q) \cong \frac{4\pi ieA\, qk}{(k^2+\eta^2)^2}. \tag{8}$$

Using Eqs. (8) and (1) one obtains

$$\frac{d\sigma_e}{d\Omega\, dE_x} = \frac{48\sqrt{2}}{\pi}\frac{e^2[e_{\rm eff}^{(1)}]^2p^2}{\hbar^2\mu c^2}\frac{1}{q^2}\frac{\sqrt{S_n}(E_x - S_n)^{3/2}}{E_x^4}. \tag{9}$$

The solid scattering angle can be related to the momentum transfer by means of $d\Omega \cong 2\pi\hbar^2 q\, dq/p^2$. The minimum momentum transfer for an excitation energy E_x is given by $q_{\rm min} = \Delta k \cong E_x/\hbar c$, so that the integral over the scattering angle yields

$$\frac{d\sigma_e}{dE_x} = 96\sqrt{2}\frac{e^2[e_{\rm eff}^{(1)}]^2}{\mu c^2}\frac{\sqrt{S_n}(E_x - S_n)^{3/2}}{E_x^4}\ln\left(\frac{pc}{E_x}\right). \tag{10}$$

Eq. (10) shows that, for large p, the energy spectrum in electro-disintegration depends weakly on the electron energy through the logarithm function. This means that there is no great advantage (in terms of number of events) in increasing the electron energy when $E_e \gg m_e c^2$. From Eq. (10) one also sees that the energy spectrum increases sharply starting at $E_x = S_n$, peaks at $E_x = 8S_n/5$, and decreases with $E_x^{-5/2}$ at large energies. This is the same characteristic spectrum as found in Coulomb dissociation of halo nuclei [12].

The integral over the excitation energy gives, to leading order,

$$\sigma_e(p) = 6\pi\sqrt{2}e^2\left[e_{\rm eff}^{(1)}\right]^2\frac{1}{\mu c^2 S_n}\ln\left(\frac{pc}{S_n}\right). \tag{11}$$

For stable nuclei, with $S_n \simeq$ few MeV, the electron-disintegration cross section is small. The dependence of Eq. (11) on the inverse of the separation energy is most important for loosely bound nuclei. Using $S_n = 100$ keV, $E_e \cong pc = 10$ MeV, $e_{\rm eff}^{(1)} = e$, and $\mu c^2 = 10^3$ MeV, Eq. (11) yields 25 mb for the dissociation cross section by high energy electrons. Note that the above equations are valid only if $E_e \gg m_e c^2$. They show that the electro-disintegration cross section increases very slowly with the electron energy. In contrast, as shown in Fig. 1, at low electron energies the cross sections increase much faster with E_e.

The arguments used here are only valid for dissociation (breakup) experiments. In the case of electron excitation of bound states, the matrix elements can become large for small excitation energies and cases where there is a large overlap of the wavefunctions. Consequently, the cross section can be much higher when these conditions are met.

3. Dissociation of halo nuclei beams on a fixed target

3.1. Dissociation by atomic electrons in the target

I use the Thomas–Fermi model to describe the electronic distribution in an atom. This approximation is well known, being described in many textbooks (see, e.g., Ref. [18]). In this model, the electron density as a function of the distance from the atomic nucleus with charge Ze is given by

$$\rho(r) = \frac{1}{3\pi^2}\left[2\frac{m_e}{\hbar^2}Ze^2\frac{\Phi(x)}{r}\right]^{3/2}, \quad \text{where}$$
$$x = br, \text{ and } b = 2\left(\frac{4}{3\pi}\right)^{2/3}\frac{m_e}{\hbar^2}e^2Z^{1/3}. \tag{12}$$

The function $\Phi(x)$ is the solution of the Thomas–Fermi equation

$$\frac{d^2\Phi}{dx^2} = \frac{\Phi^{3/2}}{x^{1/2}}. \tag{13}$$

Numerical solutions of this equation date back to Refs. [19,20]. An excellent approximation was found by Tietz [21]:

$$\Phi(x) = \frac{1}{(1+ax)^2}, \quad \text{where } a = 0.53625. \tag{14}$$

The probability density (normalized to Z) to find an electron with momentum p is given by

$$\mathcal{P}(p) = \left|D(\mathbf{p})\right|^2, \quad \text{where}$$
$$D(\mathbf{p}) = \frac{1}{(2\pi)^{3/2}}\int d^3r\, e^{i\mathbf{p}\cdot\mathbf{r}}\sqrt{\rho(r)}. \tag{15}$$

The electronic density $\rho(r)$ has to be Lorentz transformed to the frame of reference of the projectile nucleus. Assuming a straight-line projectile motion with impact parameter b from the atomic center, the transformed density is

$$\rho'(r) = \gamma\rho\left(\sqrt{b^2+\gamma^2z^2}\right), \tag{16}$$

where $\gamma = (1 - v^2/c^2)^{-1/2}$ is the Lorentz factor, and v is the projectile velocity.

The Fourier transform in Eq. (15) becomes

$$D'(\mathbf{p}) = \frac{1}{(2\pi)^{3/2}}\int d^3r\, e^{i\mathbf{p}\cdot\mathbf{r}}\sqrt{\rho'(r)}$$
$$= \frac{1}{(2\pi)^{3/2}}\frac{1}{\sqrt{\gamma}}\int d^3r'\, e^{i\mathbf{P}\cdot\mathbf{r}'}\sqrt{\rho(r')}, \tag{17}$$

where

$$\mathbf{P} = (\mathbf{p}_t, p_z/\gamma), \qquad r' = (\mathbf{b}, \gamma z), \tag{18}$$

with $\mathbf{p}_t(p_z)$ being the transverse (longitudinal) momentum.

Since $\rho(r)$ is spherically symmetric, Eq. (17) can be rewritten as

$$D'(\mathbf{p}) = \sqrt{\frac{2}{\pi\gamma}}\frac{1}{P}\int dr\, r\sin(Pr)\sqrt{\rho(r)}. \tag{19}$$

For an atom at rest, very few electrons have orbital kinetic energies larger than 100 keV. In the case of ^{92}U only 3% of the electrons (2 electrons!) have kinetic energies larger than that. But in the reference frame of a 100 MeV/nucleon projectile, 50% of the electrons have energies greater than 100 keV.

Assuming that each electron scatters independently, the total dissociation cross section by the target

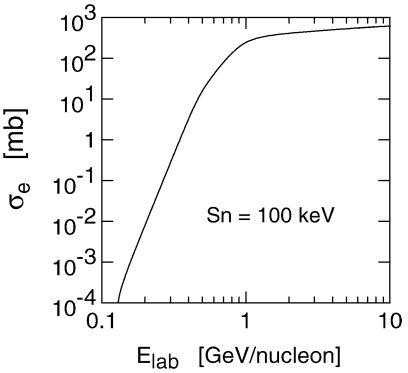

Fig. 2. Cross section for the electro-dissociation of a neutron-halo nucleus impinging on a lead target, as a function of the bombarding energy. A separation energy equal to 100 keV was used.

atomic electrons is given by

$$\sigma_e^{(\mathrm{TAE})}(p) = \int d^3p\, \mathcal{P}'(\mathbf{p})\sigma_e(p) = 2\pi \int_0^\infty dp_t\, p_t \int_{-\infty}^\infty dp_z\, \mathcal{P}'(p_z, p_t)\sigma_e(p). \tag{20}$$

The separation of the above integral into longitudinal and transverse momenta is convenient because only the longitudinal momentum component of the electrons is relevant for the dissociation of the projectile.

Fig. 2 shows the dissociation cross section for a halo nucleus, with separation energy $S_n = 100$ keV, incident on a Pb target as a function of the bombarding energy. Although the cross sections are small for incident energies equal to a few hundred MeV/nucleon, they increase drastically as the bombarding energy becomes close to 1 GeV/nucleon. At 10 GeV/nucleon the dissociation cross section is of the order of 1 barn.

Comparing the above results with those obtained in Section 2, we notice that there are different energy scales for electro-disintegration on fixed targets (by atomic electrons) and on a collider-beam mode. This is due to the Lorentz transformation and to the large density (compared to an electron beam) of electrons in a heavy atom. Thus, with beams of halo nuclei with a few GeV/nucleon one could, in principle, perform similar studies as with electron-radioactive beam colliders. The disadvantage is that the Coulomb dissociation cross sections of loosely-bound nuclei are much larger, as shown in the next section.

3.2. Coulomb dissociation

Coulomb dissociation of halo nuclei has been considered long time ago [11]. For the leading electric dipole transitions from an s- to a p-wave, the Coulomb dissociation cross section is given by [11,12]

$$\frac{d\sigma_C}{dE_x} = \frac{32}{3}\frac{Z^2e^2[e_{\mathrm{eff}}^{(1)}]^2}{\hbar^2c^2}\frac{\sqrt{S_n}(E_x - S_n)^{3/2}}{E_x^4} \times \ln\left(\frac{\gamma\hbar c}{\delta E_x R}\right), \tag{21}$$

where Z is the nuclear target charge, $\delta = 0.681\ldots$, and R is the strong interaction radius ($R \simeq R_P + R_T$). Note the similarity with Eq. (10) in the dependence on the excitation energy E_x, because the dipole operator is the same in both cases. However, the argument of the logarithm is different because of the small electron mass. Moreover, the coherent electric field of the projectile yields a factor Z^2 which substantially increases the Coulomb dissociation cross section for large-Z targets.

The total cross section for Coulomb dissociation as a function of the bombarding energy (i.e., as a function of γ) is given by

$$\sigma_C = \frac{2\pi}{3}\frac{Z^2e^2[e_{\mathrm{eff}}^{(1)}]^2}{\hbar^2c^2}\frac{\hbar^2}{\mu S_n}\ln\left(\frac{\gamma\hbar c}{\delta S_n R}\right). \tag{22}$$

Using the same values listed after Eq. (11), for 10 GeV/nucleon projectiles impinging on Pb targets, yields cross sections of approximately 24 barns. This is much larger than that due to the dissociation by electrons in the target. But the contribution of the later process comprises 5% of the total disintegration cross section, and should be considered in experimental analysis.

4. Conclusions

In this Letter the inelastic scattering of electrons off halo nuclei was studied, with emphasis on the energy dependence of the dissociation cross sections. It is shown that the cross sections for electro-dissociation of weakly-bound nuclei reach ten milibarns for 10 MeV electrons and increase logarithmically at higher energies. This means that extracting information about the continuum structure of weakly-bound

nuclei (e.g., scattering lengths and effective ranges, as in Eq. (6)) can only be done if the intensity of the radioactive beam is very large, or if the collider allows for a large number of sequential interactions between the electrons and the nuclei at different crossing points. This conclusion can be drawn from Fig. 1, where a steep decrease of the dissociation cross section with S_n is seen. Halo breakup experiments (common in fixed-target radioactive beam facilities) are difficult to carry out in electron-radioactive beam colliders, but not impossible if S_n is small.

A new facility is under construction at the GSI/Darmstadt, Germany. Experiments in a collider mode are planned so that electron beams will cross radioactive beams with center-of-mass energies of 1.5 GeV, i.e., 0.5 GeV electrons impinging on a 740 MeV/A counter propagating ion [3,22]. For light, neutron-rich, nuclei luminosities of $10^{29}/(\mathrm{cm}^2\,\mathrm{s})$ are expected. The approximate Eq. (11) yields cross sections of the order of 1 mb for $S_n \simeq 1$ MeV, what means an estimated 100 events/second.

I have also shown that electrons present in a fixed nuclear target access similar scattering conditions as in an electron-radioactive beam collider. However, Coulomb excitation cross sections are much larger in the case of a heavy nuclear target. In view of the scientific impact of an electron-radioactive beam facility these results are useful for guidance in planning future experiments. The role of electron (and photon) scattering on exotic nuclei in stellar environments is also of interest for stellar modeling and work in this direction is in progress.

Acknowledgements

I thank useful discussions with P.G. Hansen, H. Schatz, H. Simon, U. van Kolck and V. Zelevinsky. This research was supported in part by the Department of Energy under Grant No. DE-FG02-04ER41338.

References

[1] R.F. Casten, B.M. Sherrill, Prog. Part. Nucl. Phys. 45 (2000) S171.
[2] C.A. Bertulani, L.F. Canto, M.S. Hussein, Phys. Rep. 226 (1993) 281.
[3] FAIR: Facility for Antiproton and Ion Research, Conceptual Design Report, GSI, 2002, p. 162.
[4] J.M. Eisenberg, W. Greiner, Excitation Mechanisms of the Nucleus, North-Holland, Amsterdam, 1988.
[5] L.I. Schiff, Phys. Rev. 96 (1954) 765.
[6] L.J. Weigert, J.M. Eisenberg, Nucl. Phys. 53 (1964) 508.
[7] F. Scheck, Nucl. Phys. 77 (1966) 577.
[8] W.A. McKinley, H. Feshbach, Phys. Rev. 74 (1948) 1759.
[9] D.R. Yennie, D.G. Ravenhall, R.R. Wilson, Phys. Rev. 92 (1953) 1325;
D.R. Yennie, D.G. Ravenhall, R.R. Wilson, Phys. Rev. 95 (1954) 500.
[10] L.S. Cutler, Phys. Rev. 157 (1967) 885.
[11] C.A. Bertulani, G. Baur, Nucl. Phys. A 480 (1988) 615, note that a factor 1/3 is missing in Eqs. (3.2b) and (4.3b) of this reference.
[12] C.A. Bertulani, A. Sustich, Phys. Rev. C 46 (1992) 2340.
[13] T. Otsuka, et al., Phys. Rev. C 49 (1994) R2289.
[14] A. Mengoni, T. Otsuka, M. Ishihara, Phys. Rev. C 52 (1995) R2334.
[15] D.M. Kalassa, G. Baur, J. Phys. G 22 (1996) 115.
[16] S. Typel, G. Baur, Phys. Rev. Lett. 93 (2004) 142502.
[17] P.G. Hansen, B. Jonson, Europhys. Lett. 4 (1987) 409.
[18] H. Friedrich, Theoretical Atomic Physics, Springer-Verlag, Heidelberg, 1990.
[19] E.B. Baker, Phys. Rev. 36 (1930) 630.
[20] V. Bush, S.H. Caldwell, Phys. Rev. C 38 (1931) 1898.
[21] T. Tietz, J. Chem. Phys. 25 (1956) 787;
T. Tietz, Z. Naturforsch. 23a (1968) 191.
[22] H. Simon, private communication.